Resonant photoluminescence imaging and the origin of excited states in self-assembled quantum dots

T. A. Nguyen, S. Mackowski,* T. B. Hoang, H. E. Jackson, and L. M. Smith
Department of Physics, University of Cincinnati, Cincinnati, Ohio 45221-0011, USA

G. Karczewski
Institute of Physics PAS, Al. Lotników 32/46, 02-668 Warsaw, Poland

(Received 9 August 2007; revised manuscript received 2 November 2007; published 20 December 2007)

We image single quantum dot excitations using high-resolution slit-confocal microscopy in order to elucidate the nature of the excited states of single CdTe quantum dots. The results show subsets of single dots distinguished by unique excitation spectra and spatially separated by hundreds of nanometers. We conclude that the dots are superimposed on an extended two-dimensional platelet. Model simulations, which yield common resonances for two quantum dots superimposed on a microscopic wire, support this interpretation.

DOI: 10.1103/PhysRevB.76.245320 PACS number(s): 78.55.Et, 78.67.Hc, 71.35.Ji

The past decade has seen an explosion of methods to design and fabricate nanostructures with a wide degree of diversity. At the same time, a number of techniques have been developed from atomic force and electron beam microscopies[1,2] to x-ray diffraction[3] that probe the structure and morphology of these nanostructures with increasingly fine detail. As the size of these synthetic objects shrinks, the surface-to-volume ratios increase by orders of magnitude, vastly enhancing their sensitivity to local (and often uncontrolled) defects, interfaces, and morphologies. Moreover, the ability to couple nanostructures together through self- or chemical assembly adds a whole new layer of complexity.[4,5] Correlation of structural measurements with the internal electronic structure of the nanostructures has, therefore, been lagging. What is needed is the development of ways to probe the electronic structure with extremely high accuracy and at the same time provide a higher degree of sensitivity to spatial information.

In this work, we demonstrate a technique which images a macroscopic collection of nanostructures with high spatial resolution, and which can simultaneously probe *both* the ground and excited states with extremely high spectral resolution. An analysis and modeling of these results provide detailed and significant information on the spatial and electronic structures of nanoscale objects which cannot be obtained in any other way.

The imaging measurements are made on epitaxially grown CdTe semiconductor quantum dots. The sample was grown by molecular beam epitaxy on (100)-oriented GaAs substrates. Self-assembled CdTe quantum dots were formed by depositing four monolayers of CdTe by atomic layer epitaxy on a ZnTe buffer. A 50 nm thick ZnTe capping layer covered the dot layer. As estimated by transmission electron microscopy and magnetophotoluminescence measurements, the lateral size of CdTe quantum dots is of the order of 3–5 nm in diameter.[6] Further details of the sample growth and their optical characterization can be found elsewhere.[6] Our central focus is to extend advanced single dot imaging techniques[7] to understand the nature of the excited states in this structure. Previous photoluminescence and resonant Raman scattering experiments carried out on the ensemble level (with a laser spot size ~30 μm) have shown that at low temperature (T=6 K) the overall excited state distribution resembles the ground state photoluminescence (PL),[8] but it is shifted by about 100 meV toward the ZnTe barrier energy, as displayed by dashed line in Fig. 1. Notably, the total carrier confinement in these quantum dots amounts to 300 meV. Extensive optical experiments (excitation and power dependence of the PL emission) performed on the quantum dot ensemble have unambiguously demonstrated the absence of a uniform two-dimensional wetting layer.[8,9] Most frequently, the spectral signature of the wetting layer is a narrow—compared to the quantum dot (QD) emission—luminescence band located between the dot emission and the barrier which grows as a function of excitation power. Obviously, in the case of PL spectrum shown in Fig. 1, such an emission is absent, and it remains absent at significantly higher excitation powers. This feature distinguishes this quantum dot structure from most of other quantum dot systems where self-assembly has been reported.[10] In the first stage of a stan-

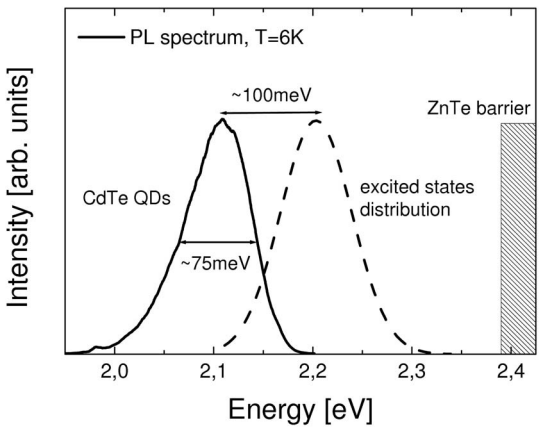

FIG. 1. Low-temperature (T=6 K) ensemble luminescence spectrum of CdTe self-assembled quantum dots (solid line). Excited state distribution (dashed line) is shifted toward higher energies by approximately 100 meV. Shaded area represents the energy of the ZnTe barrier. Note strong electronic confinement (~300 meV) of the quantum dots.

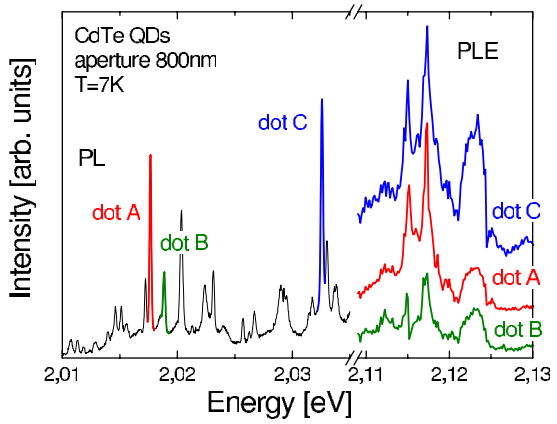

FIG. 2. (Color online) Photoluminescence excitation spectra measured for three emission lines marked with colors. The data were obtained at 7 K using 800 nm small aperture fabricated on top of the sample. The narrow resonances spaced by almost 100 meV from the detection wavelengths are virtually identical for all three quantum dots.

dard self-assembly growth of quantum dots, a uniform quantum well (the wetting layer) is formed, with a thickness which depends mainly upon the elastic properties of the two compounds and their lattice constant mismatch. The dots themselves form afterwards, on top of the wetting layer.[11] In this way, all dots in the structure are *interconnected* through the continuum of states in the wetting layer, and can be populated through direct excitation into the wetting layer.[9,12]

Here, in order to gain more information from excitation spectra, we reduce the number of QDs measured by utilizing an 800 nm aperture fabricated in a thin metal film on the top of the sample. With the laser focused on the aperture using a 50×0.5 numerical aperture microscope objective, the dots within the fixed area are examined. In Fig. 2, we show PL spectra measured at $T=7$ K for CdTe quantum dots through an aperture 800 nm in diameter together with PL excitation (PLE) spectra obtained for three single quantum dots A, B, and C, marked by colors. These excitation spectra have been obtained by scanning the laser and simultaneously taking spectra with a charge-coupled device (CCD) detector of all dots which lie within the fixed aperture. In this way, excitation spectra for multiple quantum dots could be measured at the same time. In order to achieve sufficient spectral resolution, the signal was dispersed using Dilor XY triple monochromator with a 1800 line/mm grating. The laser power was kept below 1 mW focused onto the 800 nm aperture with a 1.25 μm diameter spot. A representative spectrum (Fig. 2) shows a series of sharp PL lines emitted from the aperture which come from single quantum dots. To the right of the PL spectrum are shown the PLE spectra obtained for three of the lines marked dot A, dot B, and dot C that show the variation in intensity of each line as the excitation laser is tuned. Clearly, the excitation spectra for these lines all display similarly shaped peaks at energies of 2.114 and 2.118 eV. The energy separation between the emission lines and the excitation resonances is between 80 and 110 meV, which corresponds nicely to the excited states distribution displayed in Fig. 1. The linewidth of these resonances is

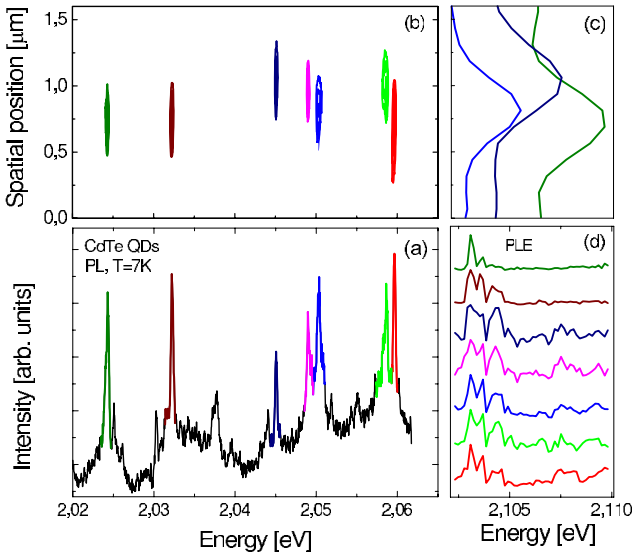

FIG. 3. (Color online) The results of photoluminescence excitation imaging experiment: (a) photoluminescence spectra showing single dot emission lines. The spatial images of the dots marked in color are shown in (b), while in (c) the cross sections along the spatial coordinate for three quantum dots are displayed. The excitation spectra measured for the seven marked single quantum dots are plotted in (d). The excitation spectra feature identical resonances although the dots are spaced from each other by several hundreds of nanometers.

limited by the spectral linewidth of the excitation dye laser, about 0.5 meV. In contrast, the width of the resonances observed in tunneling experiments on two coupled quantum dots is more than three times larger.[13] Although the observation of identical excitation resonances for QD emission lines at several different emission energies indicates the formation of a common excitation channel for these emission lines, the absence of detailed spatial information makes it impossible to distinguish between the possibilities of a single QD with several emission lines or several spatially separated single QDs emitting at different energies.

In order to provide this spatial information, we image a 400 nm$\times$6 μm region of the sample onto the entrance slit of the spectrometer using a fixed hemispherical solid immersion lens.[14,15] Applying this slit-confocal method, described in detail elsewhere,[7] we are able to directly image an array of single quantum dots on a two-dimensional CCD detector with spatial resolution of approximately 400 nm, and spectral resolution of 80 μeV. By taking a series of such images as the excitation laser is scanned, we can visualize the emission energy and spatial position of each dot, while simultaneously obtaining excitation spectra.

In Fig. 3, we show the central experimental result of this work obtained using the PL imaging technique. It shows a cluster of seven single CdTe quantum dots, which are populated through a common excited state. The main panel [Fig. 3(a)] depicts photoluminescence spectrum measured at the excitation energy of 2.103 eV with the corresponding photoluminescence map displayed in Fig. 3(b). The horizontal scale of the image is the energy, while the vertical scale represents a spatial coordinate along the slit. From the spatial

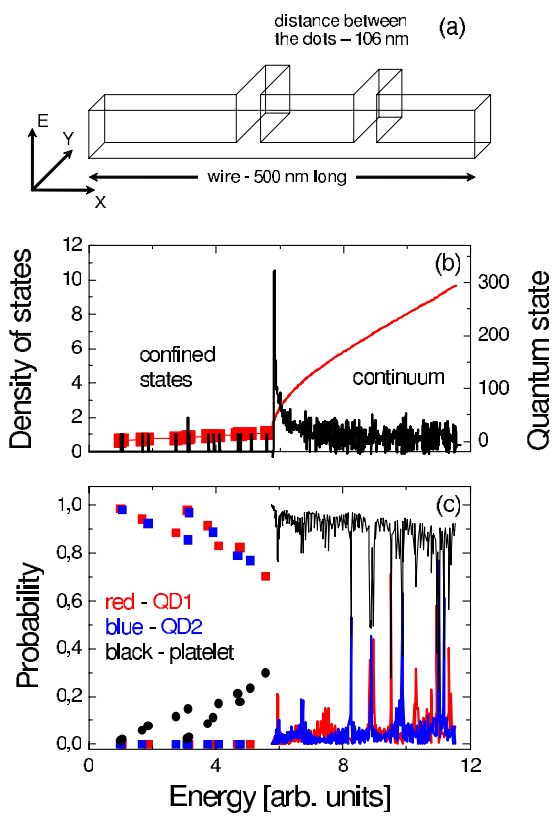

FIG. 4. (Color online) (a) Schematic drawing of the structure used for model calculations. (b) Density of states (black) and quantum state (red) dependence on the total energy of the system. Two regimes, where the carrier is confined to either of the dots or is in the continuum, are clearly distinguishable. (c) Probability of finding a particle in QD1 (red), QD2 (blue), and the platelet (black) as a function of the total energy of the system. Sharp spikes seen for energies between 8 and 12 correspond to the values where the probability of finding a particle in the dot is high.

profiles seen on the PL map, it is clear that the emission must originate from different dots. Figure 3(c) displays cross sections along the spatial axis obtained for three of the dots presented. Remarkably, despite the fact that the quantum dots seen in the image are spatially separated by as much as 500 nm, they are photoexcited through a *common excitation resonance*. This resonance is easily resolved in the very similar PLE spectra for each of the seven QDs, as shown in Fig. 3(d). Indeed, for all quantum dots within the cluster the resonances at $E=2.103$ eV and $E=2.104$ are clearly visible, although the intensities change from dot to dot. We have observed numerous examples of such clusters, comprising different numbers of quantum dots as well as featuring different energies of common resonances. The presence of various clusters exhibiting characteristic resonance energies gives additional evidence for the absence of the wetting layer in this structure. Indeed, with a wetting layer, one would expect *all* quantum dots to feature exactly the same resonance. The fact that different clusters of dots of varying size couple to unique excitation resonances suggests that clusters of very small quantum dots are formed on top of micron-sized macroscopic platelets.[16,17] Such morphology—as revealed below by simple model calculations—indeed permits electronic interaction between quantum dots separated by distances much larger than their size. The distribution of confined quantum wave functions ranges from strongly localized states within the dots at low energy, to a range of "continuum" states within the platelet, to strong resonances within the continuum of states which are quasilocalized over the dots.

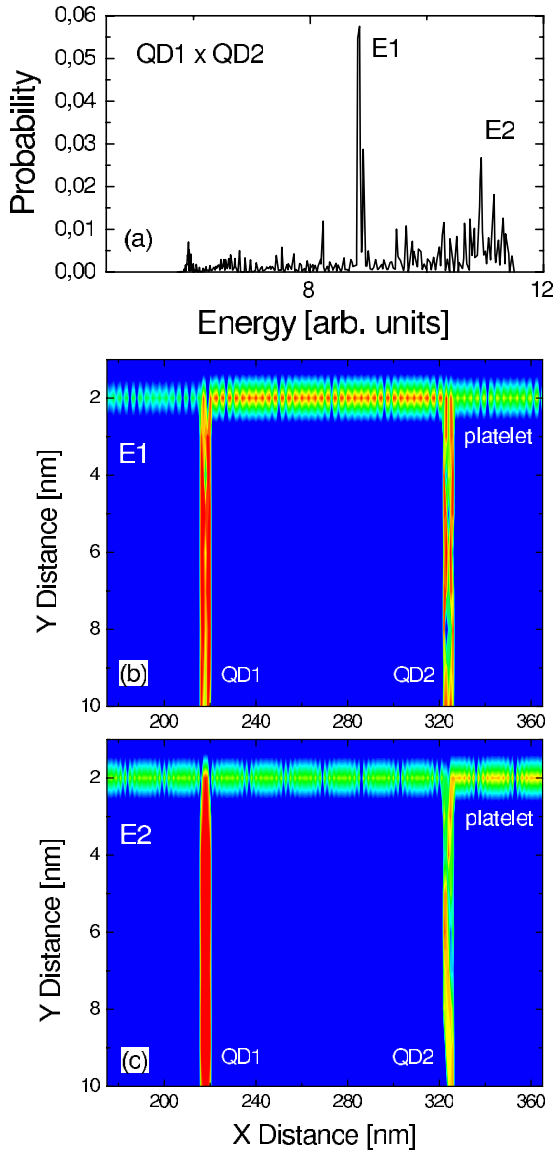

FIG. 5. (Color online) (a) Probability for finding significant probably for finding a particle in *both* QD1 and QD2 as extracted from the data shown in Fig. 4(c). The spikes correspond to energies in the continuum where there is significant probability of finding a particle in both of the dots. Corresponding wave function probabilities calculated for particle with energies (b) E1 and (c) E2, showing significant buildup of probabilities within the two quantum dots.

To model these clusters of dots, we use a one-dimensional analog of our two-dimensional system as shown in Fig. 4(a). Consider two quantum dots with sizes of 8×4 nm^2 and 7×4 nm^2 separated by 106 nm superimposed on a 500 nm long wire. Figure 4(a) is not drawn to scale in order to visu-

alize the dots. The barriers surrounding the dots and platelet are assumed to be infinite so that wave functions of free particles are completely confined within the entire structure. The Schrödinger equation is solved on a finite-element (5000 points) grid through direct inversion of a 5000×5000 matrix using MATHEMATICA. For such a system, we calculate the energy structure and the density of states that are displayed in Fig. 4(a). The red color represents the calculated eigenstate dependence on total energy of the system. The first 15 states (red symbols) are the 15 lowest discrete energy levels of the system. These states correspond to the situation when the carrier is strongly confined to the interior of the dots. When the particle is no longer confined to a dot, we obtain a continuum of states associated with the energy levels inside the wire. Similarly, in the energy dependence of the density of states (displayed in black), two regions can be easily distinguished. For the energies lower than the confinement energy of quantum dots, the density of states is composed of discrete δ-like states attributed to eigenenergies of strongly confined quantum dots. On the other hand, for energies in excess of the quantum dot potential, the density of states is characterized by $1/E$ dependence, as expected for the wire.

Using the square of the calculated wave functions, we determine the probabilities of finding a particle in either of the dots or in the platelet as a function of the total energy of the system, as displayed in Fig. 4(c). Red and blue colors represent the probabilities obtained for QD1 and QD2, respectively, while black curve and symbols correspond to the wire. Not surprisingly, for the energies below the continuum, the strongest probability is to find a particle in either dot. However, as the energy approaches the continuum threshold, the probability of finding the particle in the wire gradually increases as the wave function extends into the wirelike extended states. Importantly, in the range of localized states, a particular eigenenergy results either in finding the particle confined to QD1 or QD2, but not both. Radically different behaviors can be seen for energies within the wirelike continuum. In this case, the probabilities calculated for both the dots feature strong peaks indicating a significant probability of finding a particle *within* the dot. These peaks correlate precisely with dips in the probability dependence obtained for the wire. This is very much like the standard undergraduate problem in quantum mechanics for a one-dimensional plane wave scattering off a potential well. At particular energies, strong resonances occur which are nearly completely localized over the dot. This model calculation thus provides strong support that there exist resonances within the continuum of states in the platelet, which could extremely efficiently couple to clusters of quantum dots located upon the platelet.

In order for the two spatially separated quantum dots to couple through these above-the-barrier states, an overlap is required between the respective probabilities. In this case, for the states within the continuum, one could expect significant probability of finding the carrier in *both* QDs. In Fig. 5(a), we show the product of the probabilities calculated for QD1 and QD2. Two peaks at energies E1 and E2 are clearly distinguishable. The squares of the wave functions which correspond to these two probability resonances are displayed in Figs. 5(b) and 5(c) respectively. The wave functions associated with these two energies show a significant probability of finding a carrier in both of the quantum dots. Such a wave function would clearly result in an extremely rapid relaxation into the ground states of each dot, resulting in the strong excitation resonance we observe experimentally which couples to clusters of dots.

In summary, by combining the microscopic imaging with resonant spectroscopy of single quantum dots, we demonstrate that the morphology of the structure consists of clusters of dots that are superimposed on top of a several hundred nanometer-sized two-dimensional platelet. Such morphology provides an efficient channel for coupling between the quantum dots that can be separated by distances much larger than their sizes. These experimental results are supported by simple finite-element model calculations, which suggest that above-the-barrier states, located within the continuum of the cluster, are sufficient to allow a significant probability of transferring the excitation to either of the dots within the cluster.

The authors acknowledge the support of NSF through Grant Nos. DMR 0071797 and 0216374 (United States).

*Corresponding author. Present address: Department of Chemistry and Biochemistry, Ludwig Maximillian University, Butenandtstrasse 11, Haus E, 81377 Munich, Germany; FAX: +4989/2180-77548; sebastian.mackowski@cup.uni-muenchen.de

[1] M. Kemerink, K. Sauthoff, P. M. Koenraad, J. W. Gerritsen, H. van Kempen, and J. H. Wolter, Phys. Rev. Lett. **86**, 2404 (2001); Q. Xie, A. Madhukar, P. Chen, and N. P. Kobayashi, *ibid.* **75**, 2542 (1995).

[2] S. Bahatyrova, R. N. Frese1, C. A. Siebert, J. D. Olsen, K. O. van der Werf1, R. van Grondelle, R. A. Niederman, P. A. Bullough, C. Otto, and C. N. Hunter, Nature (London) **430**, 1058 (2004).

[3] G. Springholz, V. Holy, M. Pinczolits, and G. Bauer, Science **282**, 734 (1998); N. Krauss, W. D. Schubert, O. Klukas, P. Fromme, H. T. Witt, and N. Saenger, Nat. Struct. Biol. **3**, 965 (1996).

[4] L. Frolov, Y. Rosenwaks, Ch. Carmeli, and I. Carmeli, Adv. Mater. (Weinheim, Ger.) **17**, 2434 (2005); K. Yanagi, K. Iakoubovskii, S. Kazaoui, N. Minami, Y. Maniwa, Y. Miyata, and H. Kataura, Phys. Rev. B **74**, 155420 (2006); M. Dorogi, Z. Balint, C. Miko, B. Vileno, M. Milas, K. Hernadi, L. Forro, G. Varo, and L. J. Nagy, J. Phys. Chem. B **110**, 21473 (2006).

[5] G. Heliotis, G. Itskos, R. Murray, M. D. Dawson, I. M. Watson, and D. D. C. Bradley, Adv. Mater. (Weinheim, Ger.) **18**, 334 (2006); J. Lee, A. O. Govorov, and N. A. Kotov, Nano Lett. **5**, 2063 (2005).

[6] S. Mackowski, Thin Solid Films **412**, 96 (2002); S. Mackowski, J. Wróbel, K. Fronc, J. Kossut, F. Pulizzi, P. C. M. Christianen, J. C. Maan, and G. Karczewski, Phys. Status Solidi B **229**, 493

(2002).

[7] K. P. Hewaparakrama, A. Wilson, S. Mackowski, H. E. Jackson, L. M. Smith, G. Karczewski, and J. Kossut, Appl. Phys. Lett. **85**, 5463 (2004).

[8] T. A. Nguyen, S. Mackowski, H. E. Jackson, L. M. Smith, J. Wrobel, K. Fronc, G. Karczewski, J. Kossut, M. Dobrowolska, J. Furdyna, and W. Heiss, Phys. Rev. B **70**, 125306 (2004); A. Abdi, T. B. Hoang, S. Mackowski, L. M. Smith, H. E. Jackson, J. M. Yarrison-Rice, J. Kossut, and G. Karczewski, Appl. Phys. Lett. **87**, 183104 (2005).

[9] S. Mackowski, G. Prechtl, W. Heiss, F. V. Kyrychenko, G. Karczewski, and J. Kossut, Phys. Rev. B **69**, 205325 (2004).

[10] D. I. Lubyshev, P. P. Gonzalez-Borrero, E. Marega, E. Petitprez, N. La Scala, and P. Basmaji, Appl. Phys. Lett. **68**, 205 (1996); K. Leonardi, H. Heinke, K. Ohkawa, D. Hommel, H. Selke, F. Gindele, and U. Woggon, *ibid.* **71**, 1510 (1997); H. H. Cheng, R. J. Nicholas, D. E. Ashenford, and B. Lunn, Phys. Rev. B **56**, 10453 (1997).

[11] R. Leon and S. Fafard, Phys. Rev. B **58**, R1726 (1998).

[12] S. Sanguinetti, M. Henini, M. Grassi Alessi, M. Capizzi, P. Frigeri, and S. Franchi, Phys. Rev. B **60**, 8276 (1999); H. D. Robinson, B. B. Goldberg, and J. L. Merz, *ibid.* **64**, 075308 (2001).

[13] J. Seufert, M. Obert, G. Bacher, A. Forchel, T. Passow, K. Leonardi, and D. Hommel, Phys. Rev. B **64**, 121303(R) (2001).

[14] S. M. Mansfield and G. S. Kino, Appl. Phys. Lett. **57**, 2615 (1990); K. Karrai, X. Lorenz, and L. Novotny, *ibid.* **77**, 3459 (2000).

[15] V. Zwiller and G. J. Bjork, J. Appl. Phys. **92**, 660 (2002); S. Moehl, H. Zhao, B. Dal Don, S. Wachter, and H. Kalt, *ibid.* **93**, 6265 (2003).

[16] C. S. Kim, M. Kim, J. K. Furdyna, M. Dobrowolska, S. Lee, H. Rho, L. M. Smith, H. E. Jackson, E. M. James, Y. Xin, and N. D. Browning, Phys. Rev. Lett. **85**, 1124 (2000).

[17] C. Priester and M. Lannoo, Phys. Rev. Lett. **75**, 93 (1995).